

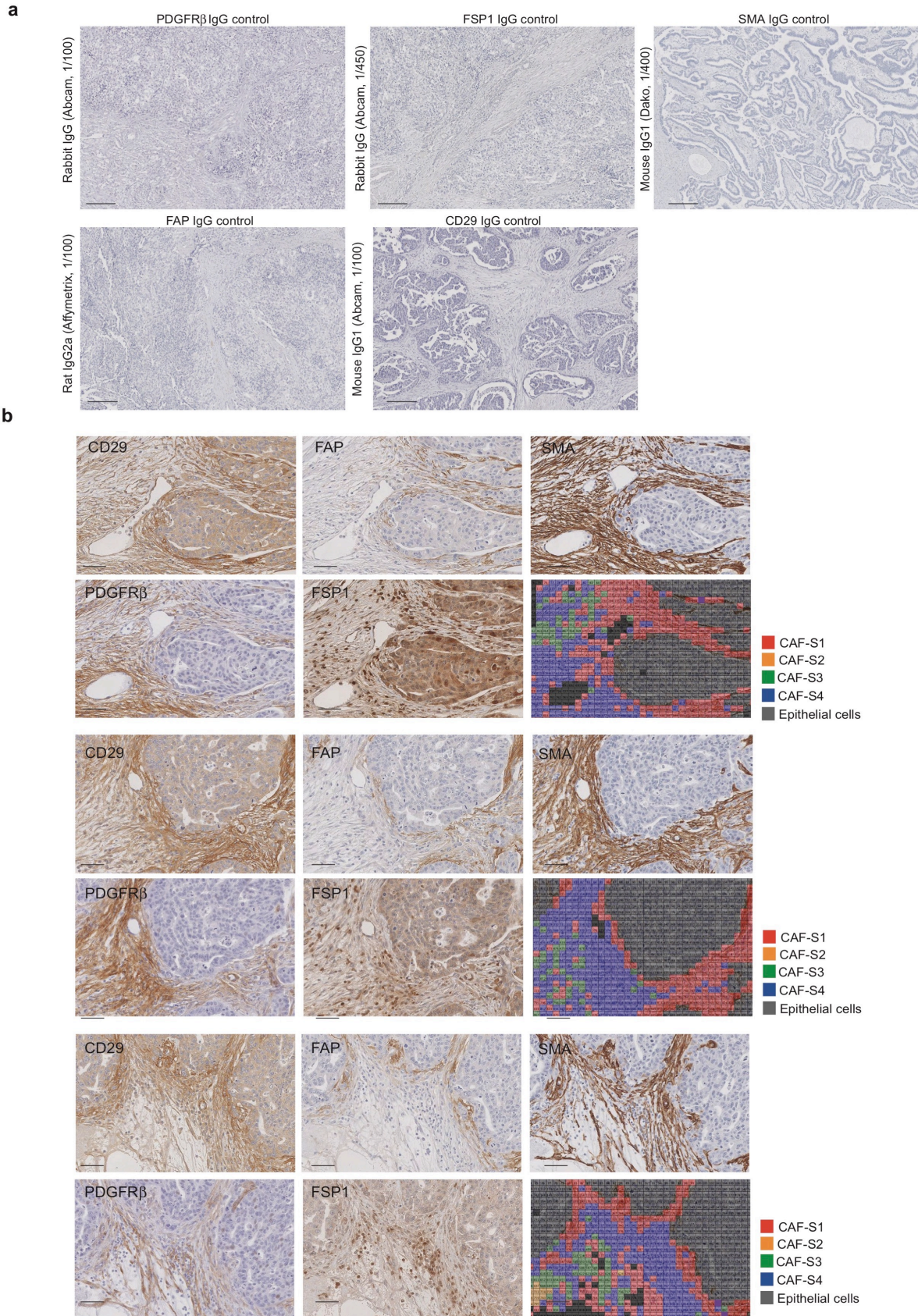
**SUPPLEMENTARY INFORMATION for**

**miR200-regulated CXCL12 $\beta$  promotes  
fibroblast heterogeneity and immunosuppression in ovarian cancers**

Anne-Marie Givel<sup>1,2</sup>, Yann Kieffer<sup>1,2</sup>, Alix Scholer-Dahirel<sup>1,2</sup>,  
Philemon Sirven<sup>1,2,3</sup>, Melissa Cardon<sup>1,2</sup>, Floriane Pelon<sup>1,2</sup>, Ilaria Magagna<sup>1,2</sup>  
Géraldine Gentric<sup>1,2</sup>, Ana Costa<sup>1,2</sup>, Claire Bonneau<sup>1,2</sup>, Virginie Mieulet<sup>1,2</sup>,  
Anne Vincent-Salomon<sup>4</sup> and Fatima Mechta-Grigoriou<sup>1,2,\*</sup>

Running title: CAF subsets and Immunosuppression in HGSOC

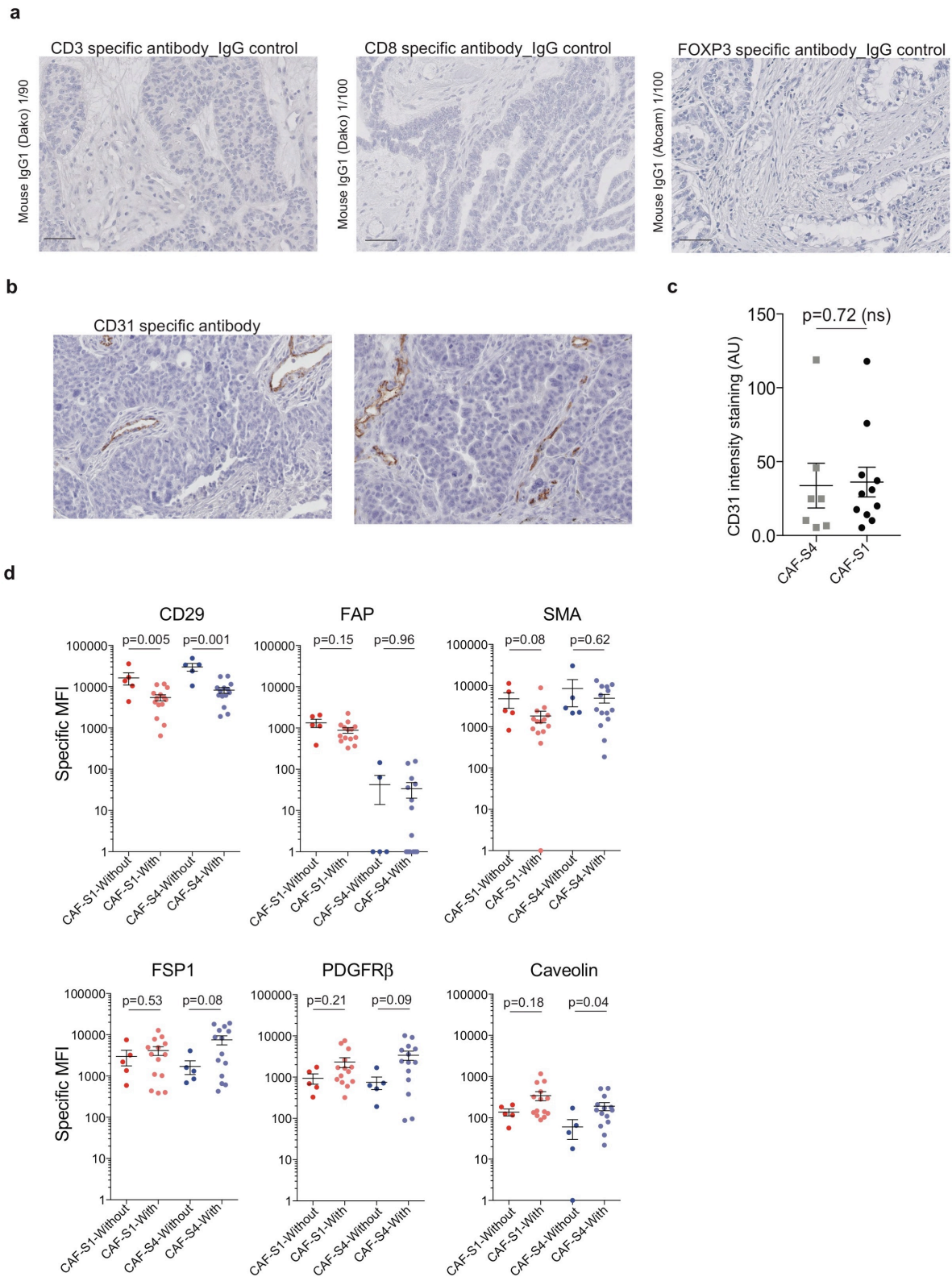
\*Corresponding author: fatima.mechta-grigoriou@curie.fr



**Supplementary Figure 1** CAF markers specificity and CAF maps from HGSOc sample patients. **a** Representative views of immunostaining performed using IgG control antibodies corresponding to the 5 CAF markers, as indicated, in the exact same conditions as used with

the corresponding specific antibodies. Scale bar = 200  $\mu\text{m}$ . **b** Maps of CAF subsets at cellular level (Bottom Right), with the corresponding views of CD29, FAP, SMA, PDGFR $\beta$  and FSP1 immunostaining of HGSOC serial sections, as indicated. For CAF maps, each square of 225  $\mu\text{m}^2$  correspond on average to a single cell and each CAF subset is represented by a color code, as indicated, with CAF-S1 in red, CAF-S2 in orange, CAF-S3 in green, CAF-S4 in blue and epithelial cells in grey. These images were reconstructed by applying mathematical modeling (see Methods) on CAF markers histological scores on serial sections. Scale bar = 200  $\mu\text{m}$ .

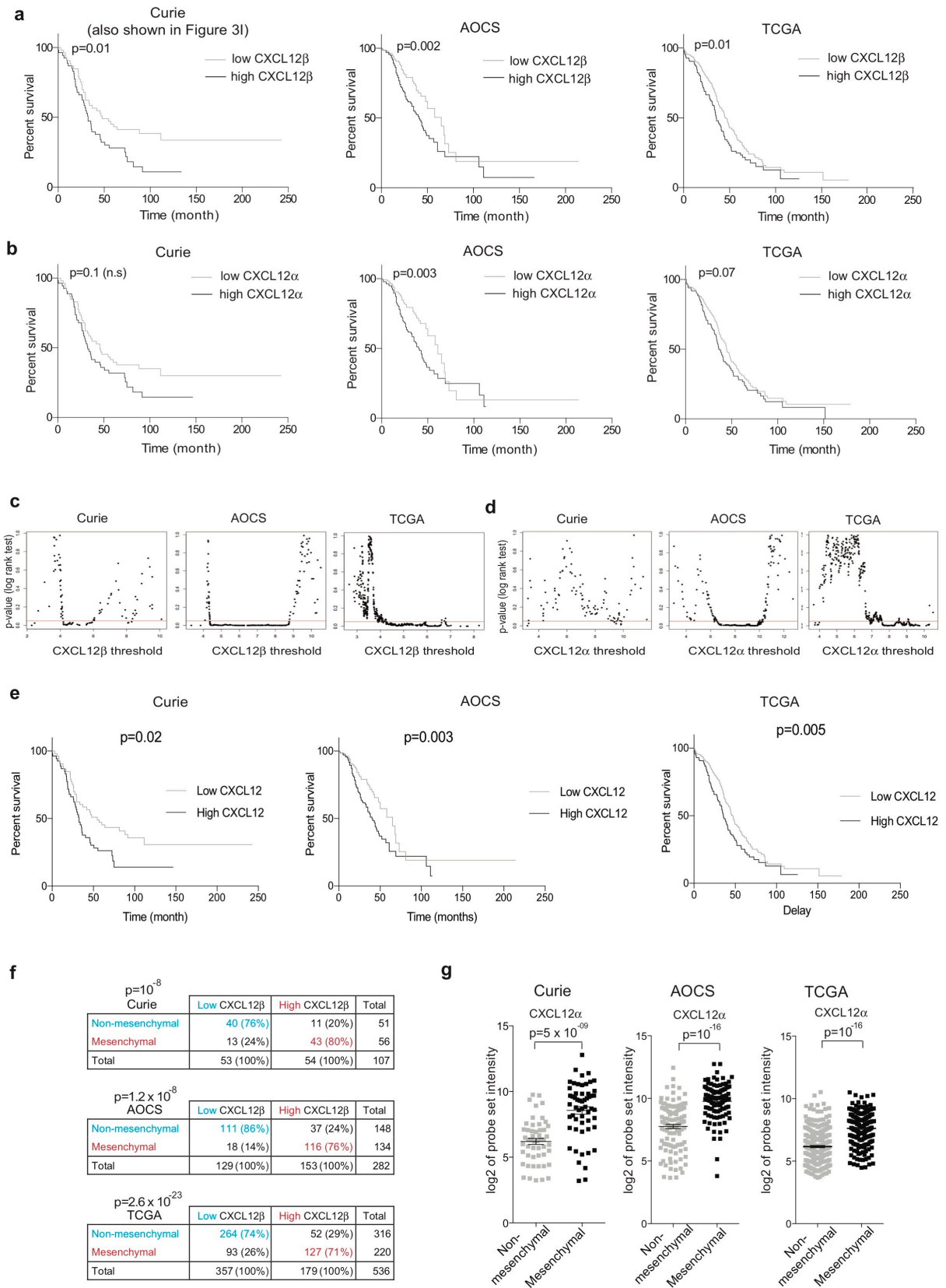




**Supplementary Figure 2** Immune antibodies specificity and vascular content in HGSOc.

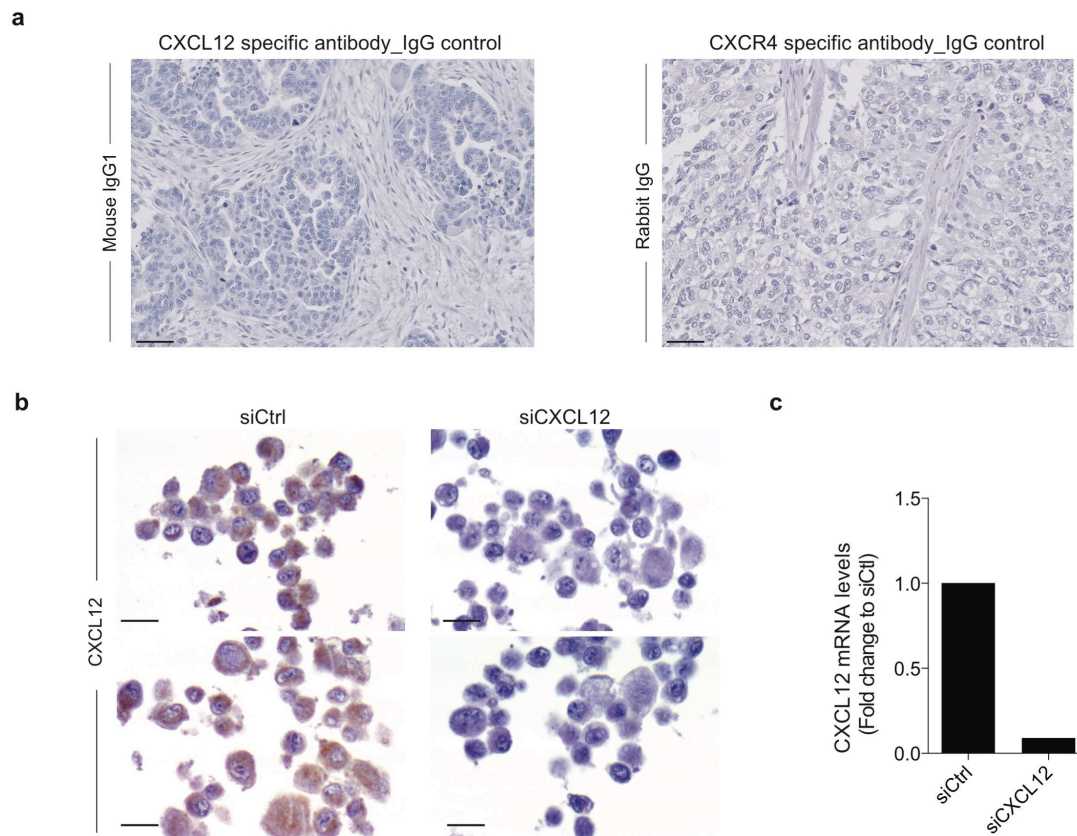
**a** Representative views of immunostaining (IHC) performed using IgG control antibodies corresponding to the immune cell markers, as indicated, in the exact same conditions as used with the corresponding specific antibodies. Scale bar = 200  $\mu$ m. **b** Representative views

of CD31+ blood vessels, detected by using CD31+ specific staining, in HGSOC sections. **c** Scatter plot showing the quantification of CD31+ blood vessels in CAF-S1 and CAF-S4 enriched HGSOC samples ( $N = 18$ ). Quantification was performed by densitometry analysis of CD31+ endothelial cells on HGSOC sections using ImageJ software. Data are shown as mean  $\pm$  SEM.  $P$  value is from Mann-Whitney test. **d** Scatter plot comparing CAF marker intensities detected in CAF-S1 and CAF-S4 subsets identified by FACS from HGSOC biopsies with or without neoadjuvant chemotherapy, as indicated. Data are expressed as specific MFI (Mean Fluorescent Intensity). Data are from 18 patients and are shown as mean  $\pm$  SEM.  $P$  values are from Mann-Whitney test.



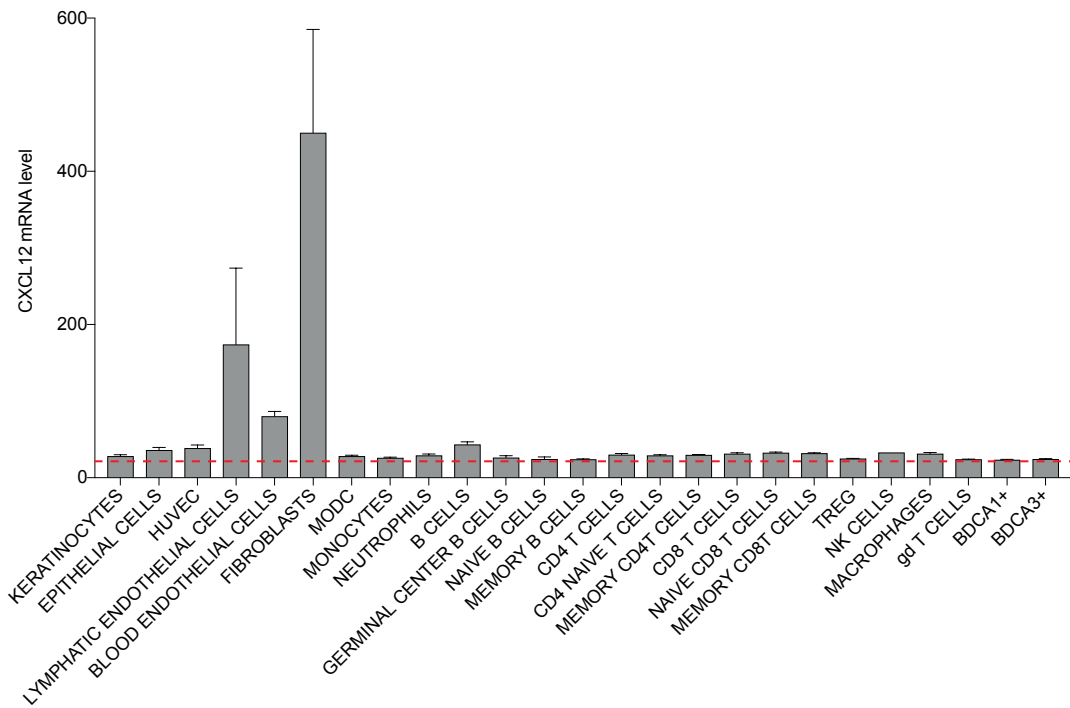
**Supplementary Figure 3** mRNA level of *CXCL12 $\beta$* , but not *CXCL12 $\alpha$* , is associated with poor survival in 3 independent cohorts of HGSOc.

**a** Kaplan-Meier curves of overall survival according to *CXCL12 $\beta$*  mRNA high and low expression using the optimal threshold determined with iteration tests (c) in Institut Curie cohort (left panel,  $N = 53$  for low-*CXCL12 $\beta$*  expression and  $N = 54$  for high-*CXCL12 $\beta$*  expression); in AOCS cohort (middle panel,  $N = 141$  for low-*CXCL12 $\beta$*  expression and  $N = 141$  for high-*CXCL12 $\beta$*  expression); and in TCGA cohort (right panel,  $N = 305$  for low-*CXCL12 $\beta$*  expression and  $N = 153$  for high-*CXCL12 $\beta$*  expression).  $P$  values are from Log-Rank test. **b** Kaplan-Meier curves of overall survival according to *CXCL12 $\alpha$*  mRNA high and low expression using the optimal threshold determined with iteration tests (d) in Institut Curie cohort (left panel,  $N = 53$  for low-*CXCL12 $\alpha$*  expression and  $N = 54$  for high-*CXCL12 $\alpha$*  expression); in AOCS cohort (middle panel,  $N = 141$  for low-*CXCL12 $\alpha$*  expression and  $N = 141$  for high-*CXCL12 $\alpha$*  expression); and in TCGA cohort (right panel,  $N = 305$  for low-*CXCL12 $\alpha$*  expression and  $N = 153$  for high-*CXCL12 $\alpha$*  expression).  $P$  values are from Log-Rank test. **c** Scatter plots showing  $P$  values of log-rank test computed by successive iterations for each threshold value of *CXCL12 $\beta$*  expression in Curie (Left), AOCS (middle) or TCGA (right) cohorts. **d** Scatter plots showing  $P$  values of log-rank test computed by successive iterations for each threshold value of *CXCL12 $\alpha$*  expression in Curie (Left), AOCS (middle) or TCGA (right) cohorts. **e** Kaplan-Meier curves of overall survival according to *CXCL12* mRNA high and low expression in Institut Curie cohort (left panel,  $N = 53$  for low-*CXCL12* expression and  $N = 54$  for high-*CXCL12* expression); in AOCS cohort (middle panel,  $N = 141$  for low-*CXCL12* expression and  $N = 141$  for high-*CXCL12* expression); and in TCGA cohort (right panel,  $N = 305$  for low-*CXCL12* expression and  $N = 153$  for high-*CXCL12* expression).  $P$  values are from Log-Rank test. **f** Contingency tables showing association between mesenchymal/non-mesenchymal and high/low-*CXCL12 $\beta$*  subgroups in HGSOC. Data are from Curi (Up), AOCS (Middle) and TCGA (Down) HGSOC patient cohorts.  $P$  values are from Fisher's Exact test. **g** Box plots showing *CXCL12 $\alpha$*  mRNA levels in mesenchymal/non-mesenchymal HGSOC from the Institut Curie, AOCS and TCGA cohorts, as indicated. Expression data are from Affymetrix U133 plus2.0 micro-arrays for Institut Curie and AOCS cohorts and from Affymetrix U133A micro-array (Level 2) for TCGA. 209687\_at probeset detects *CXCL12 $\alpha$*  mRNA. Values are expressed in log<sub>2</sub> of probeset intensity. Data are shown as mean  $\pm$  SEM.  $P$  values are from Student's t-test.

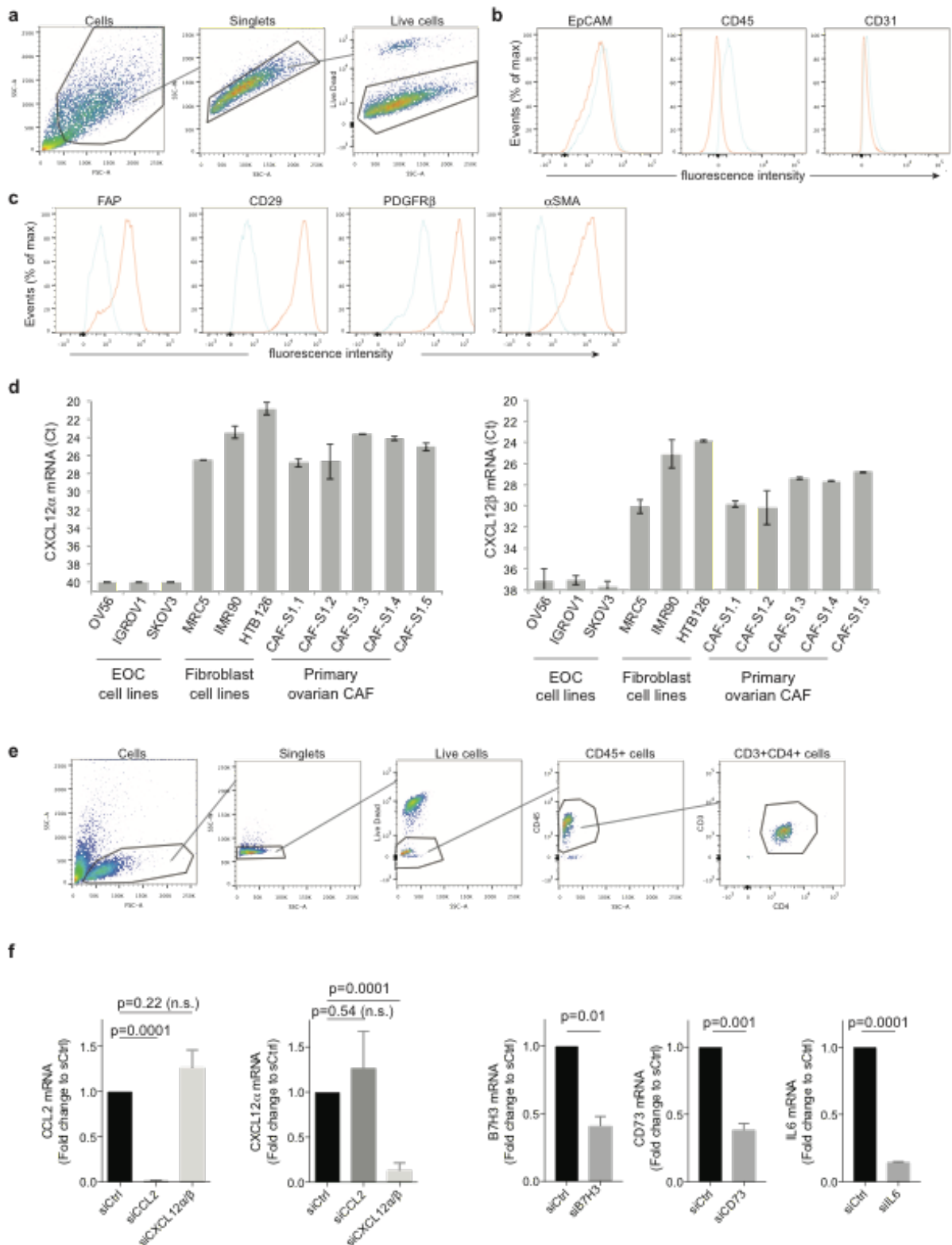


**Supplementary Figure 4** Specificity of CXCL12 and CXCR4 antibodies used for immunohistochemistry analyses of ovarian tumor sections. **a** Representative views of ovarian tumor immunostaining using IgG control antibody corresponding to CXCL12 antibody (left panel) and CXCR4 antibody (right panel). Immunostaining were performed with the exact same conditions as used for staining with CXCL12- or CXCR4-specific antibodies. Scale bar = 50  $\mu$ m. **b** Representative view of CXCL12 immunostaining on sections from paraffin-embedded fibroblast cells after transfection either with control siRNA (siCtrl, left panels) or with CXCL12-targeting siRNA (siCXCL12, right panel) in order to test the specificity of the antibody used. Scale bar = 20  $\mu$ m **c** Bar plot showing CXCL12 mRNA levels assessed by qPCR, in the same cells as in (b) to verify transfection efficiency.



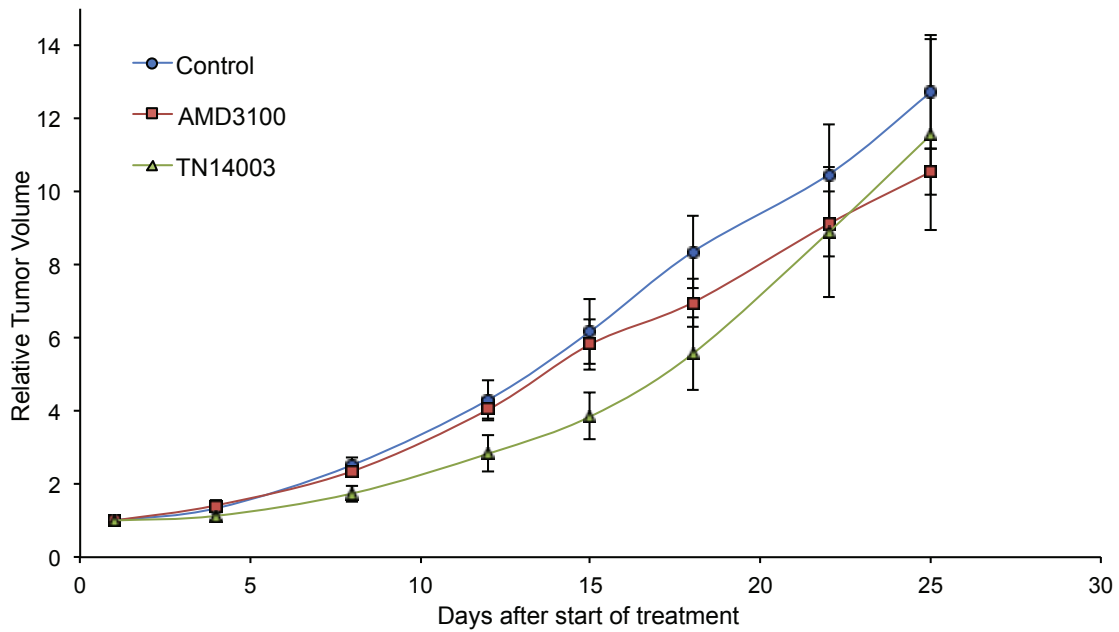


**Supplementary Figure 5** *CXCL12 $\beta$*  expression profile among different cell types. Bar plot showing *CXCL12* mRNA level in various primary cell lines, as indicated. Data have been generated from Affymetrix U133plus2.0 array and are publically available on GEO under accession number GSE49910. *CXCL12* mRNA level is shown as the average of expression of 203666\_at and 209687\_at probesets, representative of *CXCL12 $\beta$*  and *CXCL12 $\alpha$* , respectively. The red dashed line indicates limit of detection of Affymetrix U133plus2.0 array.



**Supplementary Figure 6** Characterization of human primary CAF-S1 fibroblasts and T lymphocytes. **a** Gating strategy used to characterize primary ovarian CAF. Debris and doublets were excluded based on SSC-A (side scatter), FSC-A (forward scatter) parameters,

and SSC-A, SSC-W parameters respectively. Dead cells were excluded based on their positive staining for Live/Dead marker. **b** Curves showing the fluorescence intensity detected for EPCAM, CD45 and CD31 in order to confirm that primary cells are not epithelial, hematopoietic or endothelial cells, respectively. Specific staining (red) was compared to isotype control (blue). **c** Curves showing the fluorescence intensity detected for FAP, CD29, PDGFR $\beta$  and  $\alpha$ SMA (red) markers relative to the isotype control (blue). Primary CAF expresses high level of FAP, CD29, PDGFR $\beta$  and  $\alpha$ SMA, which identify it as CAF-S1 subtype. **d** Bar plot showing *CXCL12 $\alpha$*  (Left) and *CXCL12 $\beta$*  (Right) mRNA levels in epithelial ovarian cancer cell lines, immortalized fibroblasts cell lines and primary CAF isolated from fresh HGSOC. Values are expressed in  $2^{-\Delta Ct}$ .  $n = 3$  independent experiments. Data are shown as mean  $\pm$  SEM. **e** Gating strategy for flow cytometry analysis of survival and expression of CD25 and FOXP3 in CD4 $^+$ CD25 $^-$  and CD4 $^+$ CD25 $^+$  enriched populations of T lymphocytes. Debris are first excluded based on FSC-A and SSC-A parameters, then doublets are removed, and live cells (negative for the Live/Dead staining) are further characterized for CD45, CD3 and CD4 expression.



**Supplementary Figure 7** Anti-CXCR4 treatments do not have any impact on tumor growth in a patient-derived xenograft (PDX) model of mesenchymal HGSOc. Relative tumor volume calculated over time, in PDX model of mesenchymal HGSOc. Mice were either untreated (Control, Blue line) or treated 5 days a week by intraperitoneal injection with AMD3100 (7.5mg/kg) (Red line) or TN14003 (7.5mg/kg) (Green line), as indicated. Data are shown as mean  $\pm$  SEM ( $N = 9$  to  $10$  mice per group). Tumor size was evaluated by measuring two perpendicular diameters of tumors with a caliper, twice a week until they reach ethical size. Individual tumour volumes were calculated as  $(V) = a \times b^2/2$ , with  $a$  being the major and  $b$  the minor diameter. For each tumour, the tumour volume at day  $n$  ( $V_n$ ) was reported as the initial volume before inclusion in the experiment ( $V_0$ ) and expressed as relative tumour volume (RTV) according to the following formula:  $RTV = V_n/V_0$ . Mean and standard error of the mean (s.e.m) of RTV in the same treatment group were calculated, and growth curves were established as a function of time.



<b>FACS</b>				
<b>Antibody pool for fibroblasts characterization</b>	<b>Host isotype</b>	<b>Reference</b>	<b>Dilution</b>	
PerCP/Cy5.5-EPCAM	Mouse IgG2b	Biolegend-324214	1/40	
APC/Cy7-CD45	Mouse IgG1	BD-557833	1/20	
PE/Cy7-CD31	Mouse IgG1	Biolegend-303118	1/100	
unconjugated-FAP	Mouse IgG1	R&D Systems-MAB3715	1/200	
Alexa700-CD29	Mouse IgG1	Biolegend-303020	1/100	
PE-PDGFR $\beta$	Mouse IgG1	Biolegend-323606	1/40	
<i>APC-<math>\alpha</math>SMA</i>	<i>Mouse IgG2a</i>	<i>R&amp;D Systems-IC1420A</i>	<i>1/40</i>	
<i>unconjugated-FSP1</i>	<i>Rabbit IgG</i>	<i>Abcam-ab27957</i>	<i>1/40</i>	
<i>FITC-CAVEOLIN</i>	<i>Mouse IgG2b</i>	<i>Santa Cruz-sc-70516</i>	<i>1/10</i>	
<b>IgG controls</b>		<b>Reference</b>	<b>Dilution</b>	
PerCP/Cy5.5-Mouse IgG2b		Biolegend-400338	1/40	
APC/Cy7-Mouse IgG1		BD-557873	1/20	
PE/Cy7-Mouse IgG1		Biolegend-400126	1/100	
unconjugated Mouse IgG1		R&D Systems-MAB002	1/200	
Alexa700-Mouse IgG1		Biolegend - 400144	1/100	
PE-Mouse IgG1		Biolegend - 400114	1/40	
<i>APC-Mouse IgG2A</i>		<i>R&amp;D Systems-IC003A</i>	<i>1/40</i>	
<i>unconjugated Rabbit IgG</i>		<i>Abcam-ab27472</i>	<i>1/40</i>	
<i>FITC-Mouse IgG2b</i>		<i>Santa Cruz-sc-2857</i>	<i>1/10</i>	
<b>Antibody pool for CD4+ cells characterization</b>	<b>Host isotype</b>	<b>Reference</b>	<b>Dilution</b>	
APC-CD4	Mouse IgG1	Miltenyi-130-092-374	1/20	
APC/Cy7-CD45	Mouse IgG1	BD-557833	1/20	
Alexa700-CD3	Mouse IgG1	BD-557943	1/20	
PE-CD25	Mouse IgG2b	Miltenyi-130-098-211	1/20	
PE/Cy7-CXCR4	Mouse IgG2a	Biolegend-306527	1/40	
FITC-FOXP3	Rat IgG2a	Ebioscience-11-4776-42	1/20	
<b>IgG controls</b>		<b>Reference</b>	<b>Dilution</b>	
PE-Mouse IgG2b		Miltenyi-130-092-215	1/20	
PE/Cy7-Mouse IgG2a		Biolegend-400254	1/5	
FITC-Rat IgG2a		Ebioscience-11-4321-41	1/100	
<b>Antibody pool for Treg cells sorting</b>	<b>Host isotype</b>	<b>Reference</b>	<b>Dilution</b>	
APC-CD4	Mouse IgG1	Miltenyi-130-092-374	1/20	
FITC-CD127	Mouse IgG1	ThermoFisher-11-1278-42	1/20	
PE/Cy7-CD25	Mouse IgG1	BD-557741	1/40	
PE-CD45RA	Mouse IgG2b	BD-555489	1/20	

<b>IHC</b>				
<b>Antibody against</b>	<b>Host isotype</b>	<b>Reference</b>	<b>Dilution</b>	<b>Antigen retrieval</b>
CXCL12	Mouse IgG1	R&D Systems-MAB350	1/20	EDTA pH9
CXCR4	Rabbit IgG	Epitomics-3108-1	1/50	Citrate pH6
FAP	Rat IgG2a	Vitatex-MABS1001	1/100	Citrate pH6
CD29	Mouse IgG1	Abcam-ab3167	1/100	Citrate pH6
PDGFR $\beta$	Rabbit IgG	Abcam-ab32570	1/100	Citrate pH6
$\alpha$ SMA	Mouse IgG1	Dako-M0851	1/400	Citrate pH6
FSP1	Rabbit IgG	Abcam-ab27957	1/450	Citrate pH6
CD3	Mouse IgG1	Dako-M7254	1/90	Citrate pH6
CD8	Mouse IgG1	Dako-M7103	1/100	Citrate pH6
FOXP3	Mouse IgG1	Abcam-ab20034	1/100	EDTA pH9
<b>IgG controls</b>		<b>Reference</b>		
Rabbit IgG		Abcam-ab171870		
Rat IgG2a		Affymetrix-14-4321		
Mouse IgG1		Abcam-ab91353		
Mouse IgG1		Dako-X093101		
Rabbit IgG		Dako-X090302		

**Supplementary Table 1** List of primary antibodies used in the study. List of primary antibodies used for flow cytometry (upper part), IHC and IF (lower part) analyses. For fibroblast characterization by FACS, antibodies in italic that recognize intra-cellular proteins were not added to the pool in case of analysis of fresh unfixed cells (i.e. for cell sorting). Each antibody was titrated separately to find the best concentration to use. For IHC analyses, appropriate IgG controls were used at the dilution that corresponds to the matched antibody. All antibodies recognize human proteins, and species used for antibody production is indicated.